3. Shimada H, Nabeya Y, Okazumi S, Matsubara H, Shiratori T, Gunji Y, Kobayashi S, Hayashi H, Ochiai T. Prediction of survival with squamous cell carcinoma antigen in patients with resectable esophageal squamous cell carcinoma. Surgery. 2003; 133:486–94.
4. Shimada H, Takeda A, Arima M, Okazumi S, Matsubara H, Nabeya Y, Funami Y, Hayashi H, Gunji Y, Suzuki T, Kobayashi S, Ochiai T. Serum p53 antibody is a useful tumor marker in superficial esophageal squamous cell carcinoma. Cancer. 2000;89:1677–83.
5. Shimada H, Yajima S, Oshima Y, Hiwasa T, Tagawa M, Matsushita K, Nomura F. Impact of serum biomarkers on esophageal squamous cell carcinoma. Esophagus, Inpress.
6. Mori M, Adachi Y, Matsushima T, Matsuda H, Kuwano H, Sugimachi K. Lugol staining pattern and histology of esophageal lesions. Am J Gastroenterol. 1993;88:701–5.
7. Seimiya M, Tomonaga T, Matsushita K, Sunaga M, Oh-Ishi M, Kodera Y, Maeda T, Takano S, Togawa A, Yoshitomi H, Otsuka M, Yamamoto M, Nakano M, Miyazaki M, Nomura F. Identification of novel immunohistochemical tumor markers for primary hepatocellular carcinoma; clathrin heavy chain and form imino transferase cyclo deaminase. Hepatology. 2008;48:519–30.
8. Kirchhausen T. Clathrin. Annu Rev Biochem. 2000;69:699–727.
9. Royle SJ, Lagnado L. Trimerisation is important for the function of clathrin at the mitotic spindle. J Cell Sci. 2006;119:4071–8.
10. Ohata H, Ota N, Shirouzu M, Yokoyama S, Yokota J, Taya Y, Enari M. Identification of a function-specific mutation of clathrin heavy chain (CHC) required for p53 transactivation. J Mol Biol. 2009;394:460–71.
11. Squamous cell carcinoma of the oesophagus. World Health Organization Classification of Tumours, Pathology and Genetics of Tumours of the Digestive System; 2000 pp. 11–19.
12. Dawsey SM, Lewin KJ, Wang GQ, Liu FS, Nieberg RK, Yu Y, Li JY, Blot WJ, Li B, Taylor PR. Squamous esophageal histology and subsequent risk of squamous cell carcinoma of the esophagus. A prospective follow-up study from Linxian, China. Cancer. 1994;74:1686–92.
13. Schlemper RJ, Riddell RH, Kato Y, Borchard F, Cooper HS, Dawsey SM, Dixon MF, Fenoglio-Preiser CM, Flejou JF, Geboes K, Hattori T, Hirota T, Itabashi M, Iwafuchi M, Iwashita A, Kim YI, Kirchner T, Klimpfinger M, Koike M, Lauwers GY, Lewin KJ, Oberhuber G, Offner F, Price AB, Rubio CA, Shimizu M, Shimoda T, Sipponen P, Solcia E, Stolte M, Watanabe H, Yamabe H. The Vienna classification of gastrointestinal epithelial neoplasia. Gut. 2000;47:251–5.
14. Dixon MF. Gastrointestinal epithelial neoplasia: Vienna revisited. Gut. 2002;51:130–1.
15. Wang GQ, Abnet CC, Shen Q, Lewin KJ, Sun XD, Roth MJ, Qiao YL, Mark SD, Dong ZW, Taylor PR, Dawsey SM. Histological precursors of oesophageal squamous cell carcinoma: results from a 13 year prospective follow up study in a high risk population. Gut. 2005;54:187–92.
16. Shimizu M, Nagata K, Yamaguchi H, Kita H. Squamous intraepithelial neoplasia of the esophagus: past, present, and future. J Gastroenterol. 2009;44:103–12.
17. Xu M, Jin YL, Fu J, Huang H, Chen SZ, Qu P, Tian HM, Liu ZY, Zhang W. The abnormal expression of retinoic acid receptor-beta, p 53 and Ki67 protein in normal, premalignant and malignant esophageal tissues. World J Gastroenterol. 2002;8:200–2.
18. Finlay CA, Hinds PW, Tan TH, Eliyahu D, Oren M, Levine AJ. Activating mutations for transformation by p53 produce a gene product that forms an hsc70-p53 complex with an altered half-life. Mol Cell Biol. 1988;8:531–9.
19. Bennett WP, Hollstein MC, Metcalf RA, Welsh JA, He A, Zhu SM, Kusters I, Resau JH, Trump BF, Lane DP, et al. p53 mutation and protein accumulation during multistage human esophageal carcinogenesis. Cancer Res. 1992;52:6092–7.
20. Gao H, Wang LD, Zhou Q, Hong JY, Huang TY, Yang CS. p53 tumor suppressor gene mutation in early esophageal precancerous lesions and carcinoma among high-risk populations in Henan. China. Cancer Res. 1994;54:4342–6.
21. Kobayashi M, Kawachi H, Takizawa T, Uchida K, Sekine M, Kumagai J, Momma K, Nemoto T, Akashi T, Funata N, Eishi Y, Koike M. p53 Mutation analysis of low-grade dysplasia and high-grade dysplasia/carcinoma in situ of the esophagus using laser capture microdissection. Oncology. 2006;71:237–45.
22. Gerdes J. Ki-67 and other proliferation markers useful for immunohistological diagnostic and prognostic evaluations in human malignancies. Semin Cancer Biol. 1990;1:199–206.
23. Wang WC, Wu TT, Chandan VS, Lohse CM, Zhang L. Ki-67 and ProExC are useful immunohistochemical markers in esophageal squamous intraepithelial neoplasia. Hum Pathol. 2011;42:1430–7.

Surg Today (2014) 44:859–867
DOI 10.1007/s00595-013-0622-5

ORIGINAL ARTICLE

Correlation between preoperative systemic inflammation and postoperative infection in patients with gastrointestinal cancer: a multicenter study

Yasuhiko Mohri · Chikao Miki · Minako Kobayashi · Yoshiki Okita · Mikihiro Inoue · Keiichi Uchida · Koji Tanaka · Yasuhiro Inoue · Masato Kusunoki

Received: 26 December 2012 / Accepted: 1 April 2013 / Published online: 31 May 2013

Abstract
Purpose Our aim was to examine the association between postoperative infection and preoperative systemic inflammation in patients undergoing resection of gastrointestinal cancer.
Methods We studied 862 patients who underwent elective gastrointestinal cancer surgery at six institutions. The levels of C-reactive protein and albumin were included as parameters of preoperative systemic inflammation measured using the Glasgow prognostic score. The Glasgow prognostic score was calculated based on the admission data as follows: patients with an elevated level of C-reactive protein (>1.0 mg/dl) and hypoalbuminemia (<3.5 g/dl) were allocated a score of 2, while patients showing one or none of these blood chemistry abnormalities were allocated a score of 1 or 0, respectively. The significance of the Glasgow prognostic score for predicting postoperative infection was analyzed using a multivariate analysis.
Results After surgery, 182 (21 %) patients developed postoperative infections. According to a multivariate analysis, the Glasgow prognostic score ($p < 0.01$) was independently associated with an increased risk of developing a postoperative infection. When the postoperative infections were divided into surgical site infections and remote site infections, the Glasgow prognostic score was significantly associated with an increased risk of developing remote site infections.
Conclusions Preoperative systemic inflammation is associated with postoperative infection in patients undergoing resection of gastrointestinal cancer.

Keywords Systemic inflammation · Postoperative complication · Gastrointestinal cancer

Y. Mohri (✉) · Y. Okita · M. Inoue · K. Uchida · K. Tanaka · Y. Inoue · M. Kusunoki
Department of Gastrointestinal and Pediatric Surgery, Mie University Graduate School of Medicine, 2-174 Edobashi, Tsu, Mie 5148507, Japan
e-mail: ya-mohri@clin.medic.mie-u.ac.jp

C. Miki
Department of Surgery, Iga Municipal Ueno General Hospital, Iga, Mie, Japan

M. Kobayashi · M. Kusunoki
Department of Innovative Surgery, Mie University Graduate School of Medicine, Tsu, Mie, Japan

Introduction

Patients undergoing major oncological resection are at high-risk for developing postoperative infection [1]. Recent therapeutic advances, both medical and surgical, have enabled clinicians to reduce the rate of early postoperative mortality. Despite this progress, some patients continue to have a high-risk of infection and the attendant risk of increased morbidity and mortality. Moreover, there is increasing evidence that postoperative complications due to infection following gastrointestinal cancer surgery are significantly associated with negative short- and long-term outcomes [2–4]. Many studies have reported possible risk factors for postoperative infectious complications, such as the severity of the underlying disease, an advanced age, trauma, loss of skin integrity, and malnutrition [5, 6]. Malnutrition is a common problem in surgical patients, which adversely affects the outcomes [7]. The nutritional status is evaluated based on weight loss, the serum albumin level, and the body mass index. The albumin level is the most commonly used and reliable indicator of a patient's nutritional status and is also an indicator of a negative

acute phase problem [8]. In the past decade, it has been shown that an elevated C-reactive protein (CRP) level is associated with the loss of lean body mass and increased resting energy expenditure [9, 10]. Therefore, both low albumin and high CRP levels are linked to malnutrition in oncology patients.

With regard to the measurement of the systemic inflammatory response [Glasgow prognostic score (GPS)], the combination of CRP and albumin measurement improves the prediction of cancer-specific survival in patients with a variety of common solid tumors, including stomach and colorectal cancer [11–13]. However, the relationship between preoperative systemic inflammation and postoperative infection has not been well studied. It is unknown whether a preoperative systemic inflammatory response is associated with postoperative infection in patients who have undergone gastrointestinal cancer surgery regardless of the tumor site.

The present study was conducted to evaluate preoperative systemic inflammation, as indicated by elevated CRP and low albumin levels, with respect to the prediction of postoperative infectious complications in patients with gastrointestinal cancer.

Patients and methods

A retrospective study of all patients who underwent elective gastrointestinal cancer surgery at six institutions was performed. The patients were identified using a postoperative infection database or hospital records. The data were recorded prospectively for each patient in the database immediately postoperatively by the operating surgeon. The patients were assessed for postoperative infectious complications, including surgical site infection (SSI) and remote site infection (RI), by the surgeon or attending doctor. The presence of SSI was determined according to the Centers for Disease Control and Prevention definition [14]. The definition of RI was derived from Garner and associates [15].

The subjects included in this study were patients who underwent elective surgery for stomach and/or colorectal cancer. The surgical wound class in all patients was classified as clean contaminated. Patients who did not undergo primary resection, those who had been treated with antibiotics in the past 2 weeks and those with an infection at the time of surgery were omitted from this study.

Standard procedures were used in all patients. Antimicrobial prophylaxis was administered 30 min before the procedure. The hair in the operative field was shaved using electric clippers following induction of general anesthesia. The surgical site was wiped with 10 % povidone-iodine solution before surgery and draped with a disposable towel. Absorbable synthetic sutures were used to close the fascia and peritoneum. The intra-abdominal drainage tubes were passed through a stab incision separate from the wound. The skin was closed using stainless steel staples, and the wound was then wiped with normal saline. No local irrigation of tissues with solutions containing antimicrobial agents was used. The site was kept covered with a film dressing until removal of the staples. Patients with colorectal cancer received the same protocol of mechanical bowel preparation. Routine postoperative care was provided to each patient, and each patient was followed-up for a minimum of 30 days.

The study was approved by the Ethics Review Board of each institution in which it was undertaken, and written informed consent was obtained from each patient or legal representative before entering into the study.

The data included age, sex, tumor site, operative approach, and American Society of Anesthesiologists (ASA) grade. Preoperative laboratory measurements of the white cell count and levels of hemoglobin, albumin, and CRP were obtained. The score of systemic inflammation before surgery (GPS) was estimated as previously described [16]. Briefly, patients with both an elevated CRP (>1.0 mg/dl) level and hypoalbuminemia (<3.5 g/dl) were allocated a score of 2. Patients with only one of these biochemical abnormalities were allocated a score of 1. Patients with neither of these abnormalities were allocated a score of 0.

Statistical analysis

The data are presented as the median (interquartile range). Comparisons between groups of patients were made using the Chi-square test for categorical variables and Wilcoxon rank test for continuous variables. A multiple logistic regression analysis was used to examine the effects of the variables on the development of postoperative infection, including SSI and RI. To test the independence of the risk factors, the variables found to be significant ($p < 0.1$) in the univariate analysis were entered into a multivariate logistic regression model. A p value of <0.05 was considered to be statistically significant.

Results

Data were obtained and analyzed for 862 patients who underwent elective gastrointestinal cancer surgery. There were 558 males and 304 females with 406 gastric cancers and 456 colorectal cancers. Table 1 compares the patient demographics and the incidence of postoperative infection. After surgery, 182 (21.1 %) patients developed a postoperative infection: 117 patients developed an SSI, 83

Table 1 Patient demographics

Characteristics	Total *N* (%)	Postoperative infection (−) (%)	Postoperative infection (+) (%)	*p*
Total	862	680 (78.9)	182 (21.1)	
Age, median (IQR) (years)	67 (59–74)	67 (58–74)	69 (61.5–74)	0.0487
Sex				
Male	558 (64.7)	424 (62.4)	134 (73.6)	0.0047
Female	304 (35.3)	256 (37.6)	48 (16.4)	
ASA				
Grade I	508 (59)	409 (60.1)	99 (54.4)	<0.0001
Grade II	320 (37)	255 (37.5)	65 (35.7)	
Grade III	34 (4)	16 (2.4)	18 (9.9)	
Hb, median (IQR) (g/dl)	12.2 (10.5–13.7)	12.3 (10.7–13.7)	12 (10.5–13.5)	0.0666
WBC, median (IQR) ($\times 10^9$/l)	5.9 (4.9–7.1)	5.8 (4.9–7.1)	6.1 (5.0–7.2)	0.2673
CRP, median (IQR) (mg/dl)	0.25 (0.2–0.6)	0.23 (0.2–0.5)	0.27 (0.2–1.2)	<0.0001
Alb, median (IQR) (g/dl)	3.8 (3.5–4.1)	3.8 (3.6–4.2)	3.7 (3.4–4.0)	0.0008
Time, median (IQR) (min)	240 (173–310)	230 (169–300)	272 (195.8–351.3)	<0.0001
Laparoscopic surgery				
Yes	182	5	177	0.0041
No	680	60	620	
Blood loss, median (IQR) (g)	340 (180–693)	314 (167–593.5)	546 (236.8–995.3)	<0.0001
Tumor site				
Stomach	406 (47)	332 (48.8)	74 (40.7)	0.0021
Colon	201 (23)	166 (24.4)	35 (19.2)	
Rectum	255 (30)	182 (26.8)	73 (40.1)	
R				
0	659 (76.5)	526 (77.4)	133 (73.1)	0.4804
1	59 (6.8)	45 (6.6)	14 (7.7)	
2	144 (16.7)	109 (16.0)	35 (19.2)	

ASA American Society of Anesthesiologists grade, *Hb* hemoglobin, *WBC* white blood cell count, *CRP* C-reactive protein, *Alb* albumin, *R* residual tumor classification, *IQR* interquartile range

patients developed an RI and 18 patients developed both an SSI and RI. There were significant differences between the patients with postoperative infection and the patients without postoperative infection in terms of age at the time of surgery, sex (male), a high grade of ASA, tumor site, operative time, operative approach, amount of blood loss, and the albumin and CRP levels.

The relationships between preoperative systemic inflammation (GPS) and the clinicolaboratory characteristics in the patients undergoing resection of gastrointestinal cancer are shown in Table 2. The tumor site, operative time, and amount of intraoperative blood loss did not exhibit any significant relationships with GPS. On the other hand, an increased GPS was significantly associated with an advanced age, a high ASA grade, non-curability, a high WBC count, a low hemoglobin level, and the incidence of postoperative infection and RI.

The results of the univariate analyses of postoperative infection, using the same factors as those shown in Table 1, are presented in Table 3. Sex and the ASA grade, tumor site, laparoscopic surgery, operative time, amount of blood loss, and GPS were associated with postoperative infection. The multivariate analyses revealed that sex (male) and the GPS, ASA grade, tumor site, operative time, and amount of blood loss were independently associated with an increased risk of developing a postoperative infection (Table 3). The GPS was also an independent factor for the development of postoperative infectious complications in each tumor site when the data were analyzed according to the tumor site (gastric cancer and colorectal cancer).

The relationships between SSI and the clinicolaboratory characteristics, including preoperative systemic inflammation, are shown in Table 4. According to the univariate logistic regression analysis, sex (male) and the tumor site (rectum), laparoscopic surgery, operative time, and amount of blood loss were associated with an increased risk of developing an SSI. According to the multivariate analysis, the tumor site and amount of blood loss were independently

Table 2 Relationships between clinicolaboratory characteristics and GPS

	GPS 0 ($N = 616$)	GPS 1 ($N = 160$)	GPS 2 ($N = 86$)	p
Age (years)				
<60	188 (78.3)	33 (13.8)	19 (7.9)	0.0006
60–75	330 (72.5)	80 (17.6)	45 (9.9)	
>75	98 (58.7)	47 (28.1)	22 (13.2)	
Sex				
Male	408 (73.1)	92 (16.5)	58 (10.4)	0.1028
Female	208 (68.4)	68 (22.4)	28 (9.2)	
ASA				
I	382 (75.2)	85 (16.7)	41 (8.1)	0.0014
II	217 (67.8)	67 (20.9)	36 (11.3)	
III	17 (50)	8 (23.5)	9 (26.5)	
Site of tumor				
Gastric cancer	291 (71.7)	74 (18.2)	41 (10.1)	0.9692
Colorectal cancer	325 (71.3)	86 (18.9)	45 (9.9)	
R				
R0	504 (76.5)	112 (17)	43 (6.5)	<0.0001
R1	40 (67.8)	13 (22)	6 (10.2)	
R2	72 (50)	35 (24.3)	37 (25.7)	
WBC				
<5000/mm^3	187 (78.9)	42 (17.7)	8 (3.4)	<0.0001
5000–7000/mm^3	296 (74.4)	72 (18.9)	30 (7.5)	
>7000/mm^3	133 (58.6)	46 (20.3)	48 (21.2)	
Hb				
<10 g/dl	65 (38.7)	49 (29.2)	54 (32.1)	<0.0001
10–14 g/dl	400 (75.1)	105 (19.6)	28 (5.3)	
>14 g/dl	151 (93.8)	6 (3.7)	4 (2.5)	
Operation time				
<170 min	150 (71.1)	39 (18.5)	22 (10.4)	0.9341
170–300 min	304 (72.8)	75 (17.9)	39 (9.3)	
>300 min	162 (69.5)	46 (19.7)	25 (10.7)	
Blood loss				
<180 ml	161 (73.9)	37 (17)	20 (9.2)	0.1874
180–700 ml	317 (73)	80 (18.4)	37 (8.5)	
>700 ml	138 (65.7)	43 (20.5)	29 (13.8)	
Postoperative infection				
Yes	112 (61.5)	42 (23.1)	28 (15.4)	0.0020
No	504 (74.1)	118 (17.4)	58 (8.5)	
Surgical site infection				
Yes	77 (65.8)	25 (21.4)	15 (12.8)	0.3204
No	539 (72.4)	135 (15.7)	71 (9.5)	
Remote site infection				
Yes	44 (53)	22 (26.5)	17 (20.5)	0.0001
No	572 (73.4)	138 (17.7)	69 (8.9)	

ASA American Society of Anesthesiologists grade, *R* residual tumor classification, *WBC* white blood cell count, *Hb* hemoglobin

associated with an increased risk of developing an SSI. When the data were analyzed according to the two tumor sites, the extent of gastrectomy (total gastrectomy) was found to be the only independent factor for the development of SSI in the patients undergoing gastric cancer surgery. In contrast, a male gender and the amount of blood loss were found to be independent factors for the development of SSI in the patients undergoing colorectal cancer surgery.

The relationships between RI and the clinicolaboratory characteristics are shown in Table 5. According to the

Table 3 Relationships between the studied variables and postoperative infection in patients treated with gastrointestinal cancer surgery

	Overall				Gastric cancer				Colorectal cancer			
	Univariate	Multivariate			Univariate	Multivariate			Univariate	Multivariate		
	p	RR	95 % CI	*p*	*p*	RR	95 % CI	*p*	*p*	RR	95 % CI	*p*
Age (<60/60–75/ >75 years)	0.10				0.31				0.18			
Sex (female/male)	0.004	1.64	1.11–2.45	0.01	0.69				0.0002	2.09	1.27–3.50	0.003
ASA (I/II/III)	0.006	2.27	1.26–4.07	0.006	0.003	4.03	1.62–10.24	0.003	0.25			
GPS (0/1/2)	0.001	1.89	1.11–3.21	0.02	0.007	2.43	1.10–5.33	0.03	0.03	2.25	1.14–2.10	0.02
Hb (>14/10–14/ <10 g/dl)	0.07	1.32	0.70–2.48	0.39	0.03	0.90	0.57–2.45	0.83	0.77			
WBC (<5.0/5.0–7.0/ >7.0 × 10^3/mm^3)	0.36				0.99				0.26			
Tumor site (stomach/colon/ rectum)	0.003	1.92	1.29–2.88	0.001	–	–	–	–	–	–	–	–
R (R0/R1/R2)	0.24				0.04	1.05	0.50–2.12	0.90	0.90			
Laparoscopic surgery (yes/no)	0.002	0.50	0.17–1.20	0.13	0.047	0.74	1.36–2.10	0.59	0.03	0.42	0.02–2.25	0.36
Operation time (<170/170–300/ >300 min)	<0.001	2.13	1.13–4.04	0.02	0.005	1.58	0.59–4.31	0.36	<0.0001	1.60	0.67–3.87	0.29
Blood loss (<180/ 180–700/ >700 ml)	<0.001	2.30	1.20–4.45	0.01	0.002	1.05	0.37–2.98	0.93	<0.0001	2.97	1.22–2.23	0.02
Total gastrectomy	–	–	–	–	<0.0001	3.41	1.85–5.33	<0.001	–	–	–	–
Rectal surgery	–	–	–	–	–	–	–	–	0.005	1.31	0.77–2.23	0.32

ASA American Society of Anesthesiologists grade, *GPS* Glasgow prognostic score, *Hb* hemoglobin, *WBC* white blood cell count, *R* residual tumor classification, *RR* risk ratio, *95 % CI* 95 % confidence interval

univariate logistic regression analysis, an advanced age, sex (male), the ASA grade, a low hemoglobin level, the amount of blood loss, and the GPS were associated with an increased risk of developing an RI. According to the multivariate analysis, an advanced age, sex (male) and the GPS were independently associated with an increased risk of developing an RI. Among the patients undergoing gastric cancer surgery, the ASA grade, GPS, and extent of gastrectomy were independent factors for the development of RI. Among the patients undergoing colorectal cancer surgery, an advanced age and the amount of blood loss, but not the GPS, were independent factors for the development of RI.

Discussion

Our study based on individual data for 862 patients undergoing resection for gastrointestinal cancer demonstrated that preoperative systemic inflammation (GPS) is independently associated with an increased risk of postoperative infection. Given that postoperative infections are relatively common in patients undergoing gastrointestinal surgery and are associated with increased hospital stays and treatment costs, it is possible that the simple routine preoperative measurement of the GPS is clinically useful in identifying patients at high-risk of developing infections. To the best of our knowledge, few studies have evaluated common risk factors for postoperative infections in patients undergoing various gastrointestinal cancer surgeries. The primary advantage of this study is that a significant number of patients had data for prospective postoperative infection surveillance. Furthermore, this was a multicenter study that included private medical centers, institutional hospitals, and university hospitals. Therefore, our results are more representative of oncological surgical practice, avoiding the bias of single center recruitment.

Resection of gastrointestinal cancer is associated with a high rate of postoperative infections, ranging from 20 to 40 % [1]. Recent advances in both surgical techniques and perioperative care have led to a reduction in morbidity and mortality following gastrointestinal cancer surgery. Despite these advances, infectious complications still pose a major clinical problem, particularly in high-risk patient populations. Previous studies have shown that the clinical diagnosis of a complicated postoperative course may be

Table 4 Relationships between the studied variables and surgical site infection in patients treated with gastrointestinal cancer surgery ($n = 862$)

	Overall				Gastric cancer				Colorectal cancer			
	Univariate	Multivariate			Univariate	Multivariate			Univariate	Multivariate		
	p	RR	95 % CI	*p*	*p*	RR	95 % CI	*p*	*p*	RR	95 % CI	*p*
Age (<60/60–75/ >75 years)	0.7602				0.99				0.73			
Sex (female/male)	0.0274	1.437	0.922–2.285	0.1102	0.99				0.002	1.90	1.07–3.52	0.03
ASA (I/II/III)	0.2069				0.08	1.59	0.93–2.70	0.09	0.74			
GPS (0/1/2)	0.1441				0.90				0.052	2.12	0.97–4.60	0.06
Hb (>14/10–14/ <10 g/dl)	0.5144				0.77				0.74			
WBC (<5.0/ 5.0–7.0/ >7.0 × 10^3/ mm^3)	0.2044				0.49				0.04	1.56	0.73–3.41	0.25
Tumor site (stomach/colon/ rectum)	0.0005	2.038	1.138–1.796	0.0021	–	–	–	–	–	–	–	–
R (R0/R1/R2)	0.8851				0.99				0.91			
Laparoscopic surgery	0.0134	0.475	0.112–1.368	0.1843	0.096	0.53	0.08–2.00	0.39	0.16			
Operation time (<170/170–300/ >300 min)	<0.0001	2.097	0.996–4.493	0.0527	0.002	2.67	0.79–9.50	0.11	<0.0001	1.30	0.47–3.64	0.61
Blood loss (<180/ 180–700/ >700 ml)	<0.0001	2.828	1.303–6.215	0.0084	0.003	1.39	0.39–5.06	0.61	<0.0001	3.73	1.33–10.76	0.01
Total gastrectomy (yes/no)	–	–	–	–	0.0005	2.35	1.15–4.89	0.02	–	–	–	–
Rectal surgery (yes/no)	–	–	–	–	–	–	–	–	0.003	1.59	0.86–3.03	0.14

ASA American Society of Anesthesiologists grade, *GPS* Glasgow prognostic score, *Hb* hemoglobin, *WBC* white blood cell count, *R* residual tumor classification, *RR* risk ratio, *95 % CI* 95 % confidence interval

significantly delayed, with the median time to diagnosis occurring on day 8 [17]. Preoperatively identifying patients at risk of postoperative infections may affect surgical management modifications, and thus reduce mortality associated with infectious morbidities.

Previous research has indicated that an advanced patient age, comorbidities, longer operative times, malnutrition, and the use of blood transfusions are associated with a high rate of postoperative infection. Malnutrition is common among oncology patients and leads to a reduction in the performance status and quality of life [5, 6]. The presence of systemic inflammation, as indicated by an increased CRP level and a decreased albumin level, is associated with weight loss in patients with various solid tumors [18–20]. Therefore, both high CRP and low albumin levels are linked to malnutrition. To date, there are few data in the literature regarding the effects of preoperative systemic inflammation on the development of postoperative infection. Recently, Moyes et al. [21] reported an independent association between systemic inflammation and postoperative infection following curative resection of colorectal cancer. However, the precise role of preoperative systemic inflammation in the development of postoperative infection is unclear. The current study showed that the GPS can be used to identify patients at an increased risk for infection following resection of gastrointestinal tumors, regardless of the tumor site. We also investigated the impact of the GPS on the development of postoperative infection according to the tumor site. A significant association between the GPS and the development of postoperative infection was observed with respect to both tumor sites. Therefore, we confirmed that preoperative systemic inflammation, as evidenced by the GPS, is an independent factor for the development of postoperative infection, regardless of the tumor site.

Postoperative infections are usually classified as SSIs or RIs. SSIs and RIs may have a distinct pathogenesis, being specific to different underlying mechanisms, and may

Table 5 Relationships between the studied variables and remote site infection in patients treated with gastrointestinal cancer surgery ($n = 862$)

	Overall				Gastric cancer				Colorectal cancer			
	Univariate	Multivariate			Univariate	Multivariate			Univariate	Multivariate		
	p	RR	95 % CI	*p*	*p*	RR	95 % CI	*p*	*p*	RR	95 % CI	*p*
Age (<60/60–75/>75 years)	0.0007	2.805	1.255–6.491	0.0116	0.053	1.92	0.79–2.46	0.26	0.005	2.27	1.38–3.83	0.001
Sex (female/male)	0.0200	1.757	1.025–3.122	0.0402	0.25				0.04	1.91	0.95–4.12	0.07
ASA (I/II/III)	0.0022	1.675	0.692–3.900	0.2477	0.005	1.89	1.00–3.51	0.049	0.12			
GPS (0/1/2)	<0.0001	2.305	1.143–4.597	0.0199	<0.0001	2.17	1.63–3.69	0.004	0.14			
Hb (>14/10–14/<10 g/dl)	0.0209	1.378	0.579–3.289	0.4690	0.01	0.79	0.40–3.69	0.50	0.37			
WBC (<5.0/5.0–7.0/>7.0 × 10^3/mm^3)	0.5328				0.71				0.60			
Tumor site (stomach/colon/rectum)	0.9421				–	–	–	–	–	–	–	–
R (R0/R1/R2)	0.0884	1.252	0.683–2.225	0.4584	0.003	1.32	0.85–4.02	0.21	0.57			
Laparoscopic surgery	0.2954				0.37				0.54			
Operation time (<170/170–300/>300 min)	0.0550	1.764	0.747–4.337	0.1957	0.28				0.11			
Blood loss (<180/180–700/>700 ml)	0.0237	1.500	0.631–3.594	0.3589	0.20				0.06	2.71	1.11–6.80	0.03
Total gastrectomy (yes/no)	–	–	–	–	0.003	2.90	1.39–6.21	0.005	–	–	–	–
Rectal surgery (yes/no)	–	–	–	–	–	–	–	–	0.53			

ASA American Society of Anesthesiologists grade, *GPS* Glasgow prognostic score, *Hb* hemoglobin, *WBC* white blood cell count, *R* residual tumor classification, *RR* risk ratio, *95 % CI* 95 % confidence interval

differ from each other with respect to risk factors. It is important to identify which clinical and laboratory factors can predict site-specific patterns of postoperative infection in patients with SSIs and RIs, as this information may assist surgeons in developing specific strategies to prevent infection according to an oncology patient's risk factors. Previous studies have not evaluated whether the presence of preoperative systemic inflammation can be used to predict site-specific patterns of postoperative infection [21]. In the present study, we examined site-specific risk factors for SSIs and RIs in gastrointestinal cancer patients. We found that the tumor site (rectum) and amount of blood loss were independently associated with the development of SSI, whereas the GPS and sex (male) were independently associated with the development of RI. Similar to the findings of previous reports [4, 22], our results showed that the risk factors for SSI and RI are different. With respect to the development of RI, the GPS was found to be an independent risk factor in the patients undergoing gastric cancer surgery, but not in those undergoing colorectal cancer surgery. Although the association between the GPS and RI observed in the patients undergoing colorectal cancer surgery was not significant, there was a higher incidence of RI among the patients with an elevated GPS (GPS0 8 %, GPS1 12.8 %, and GPS2 13.3 %). An evaluation of a larger cohort is needed to determine whether preoperative systemic inflammation is an indicator of site-specific infection in each tumor site.

The basis of the independent relationship between an increased GPS before surgery and postoperative infection in patients with gastrointestinal cancer is unclear. The increased CRP levels observed in oncology patients may be due to the increased production of proinflammatory cytokines by tumors or tissue necrosis. Indeed, the serum IL-6 levels have been shown to be closely correlated with the CRP levels in patients with gastrointestinal cancer [23–25]. On the other hand, a decrease in the albumin level from 4.5 to 2.1 g/dl is associated with an increase in morbidity from

10 to 65 % [26]. Hypoalbuminemia is associated with impairment of the innate immune response; hypoalbuminemia is known to cause impairment of macrophage activation and induce macrophage apoptosis [27, 28]. Moreover, parallel to the increase in the CRP level, a decrease in the albumin level has been observed and verified in patients with various types of tumors [29, 30]. Therefore, the presence of a systemic inflammatory response, as evidenced by an elevated CRP level and hypoalbuminemia, reflects the host's immune dysfunction and should be routinely evaluated in blood chemistry examinations before surgery.

There are no studies regarding the treatment of preoperative systemic inflammation in patients with solid tumors. As mentioned above, the presence of systemic inflammation in oncology patients is closely related to the upregulation of interleukins, particularly IL-6, and impairment of the innate immune system. Identifying the mechanisms underlying the development of preoperative systemic inflammation in cancer patients could help to prevent postoperative infections. Further research is needed to determine whether preoperative systemic inflammation is a reversible phenomenon.

In summary, the results of this study indicate that a simple inflammation-based prognostic score can be used to identify patients at an increased risk of developing infectious complications following resection of gastrointestinal cancer.

Acknowledgments The following investigators assisted in this study: T. Iwnaga and T. Masuda (Kuwana City Hospital), T. Kitagawa and S. Umegae (Yokkaichi Social Insurance Hospital, Mie), T. Ikeda and H. Tonouchi (Mie Prefecture Medical Center, Mie), H. Urata and T. Fukuura (Iga Municipal Ueno General Hospital, Mie), T. Mohri and T. Kato (Toyama Hospital, Mie) and M. Ohi and J. Hiro (Mie University Hospital, Mie).

Conflict of interest No commercial sponsorship was obtained or used in the collection of data, interpretation of data or analysis of this manuscript. The authors have no conflicts of interest to declare.

References

1. Velasco E, Thuler LC, Marins CA, Dias LM, Goncalves VM. Risk factors for infectious complications after abdominal surgery for malignant disease. Am J Infect Control. 1996;24:1–6.
2. Kashimura N, Kusachi S, Konishi T, Shimizu J, Kusunoki M, Oka M, et al. Impact of surgical site infection after colorectal surgery on hospital stay and medical expenditure in Japan. Surg Today. 2012;42:639–45.
3. Tsujimoto H, Ichikura T, Ono S, Sugasawa H, Hiraki S, Sakamoto N, et al. Impact of postoperative infection on long-term survival after potentially curative resection for gastric cancer. Ann Surg Oncol. 2009;16:311–8.
4. McArdle CS, McMillan DC, Hole DJ. Impact of anastomotic leakage on long-term survival of patients undergoing curative resection for colorectal cancer. Br J Surg. 2005;92:1150–4.
5. Tang R, Chen HH, Wang YL, Changchein CR, Chen JS, Hsu KC, et al. Risk factors for surgical site infection after elective resection of the colon and rectum: a single-center prospective study of 2,809 consecutive patients. Ann Surg. 2001;234:181–9.
6. Pessaux P, Msika S, Atalla D, Hay JM, Flamant Y, French Association for Surgical Research. Risk factors for postoperative infectious complications in noncolorectal abdominal surgery. A multivariate analysis based on a prospective multicenter study of 4718 patients. Arch Surg. 2003;138:314–24.
7. Sungurtekin H, Sungurtekin U, Balci C, Zencir M, Erdem E. The influence of nutritional status on complications after major intraabdominal surgery. J Am Coll Nutr. 2004;23:227–32.
8. Sung J, Bochicchio GV, Joshi M, Bochicchio K, Costas A, Tracy K, et al. Admission serum albumin is predictive of outcome in critically ill trauma patients. Am Surg. 2004;70:1099–102.
9. Al-shaiba R, McMillan DC, Angerson WJ, Leen E, McArdle CS, Horgan P. The relationship between hypoalbuminemia, tumour volume and the systemic inflammatory response in patients with colorectal liver metastases. Br J Cancer. 2004;91:205–7.
10. Deans DA, Tan BH, Wigmore SJ, Ross JA, de Beaux AC, Paterson-Brown S, et al. The influence of systemic inflammation, dietary intake and stage of disease on rate of weight loss in patients with gastro-oesophageal cancer. Br J Cancer. 2009;100:63–9.
11. McMillan DC. An inflammation-based prognostic score and its role in the nutrition-based management of patients with cancer. Proc Nutr Soc. 2008;67:257–62.
12. McMillan DC, Crozier JE, Canna K, Angerson WJ, McArdle CS. Evaluation of an inflammation-based prognostic score (GPS) in patients undergoing resection for colon and rectal cancer. Int J Colorectal Dis. 2007;22:881–6.
13. Ishizuka M, Nagata H, Takagi K, Horie T, Kubota K. Inflammation-based prognostic score is a novel predictor of postoperative outcome in patients with colorectal cancer. Ann Surg. 2007;242:326–41.
14. Mangram AJ, Horan TC, Pearson ML, Silver LC, Jarvis WR. Guideline for prevention of surgical site infection, 1999 Centers for Disease Control and Prevention (CDC) Hospital Infection Control Practices Advisory Committee. Am J Infect Control. 1999;27(2):97–132.
15. Garner JS, Jarvis WR, Emori TG, Horan TC, Hughes JM. CDC definitions for nosocomial infections, 1988. Am J Infect Control. 1988;16:128–40.
16. Crumley AB, McMillan DC, McKernan M, McDonald AC, Stuart RC. Evaluation of an inflammation-based prognostic score in patients with inoperable gastro-oesophageal cancer. Br J Cancer. 2006;94:637–41.
17. Smyth ET, Emmerson AM. Surgical site infection surveillance. J Hosp Infect. 2000;45:173–84.
18. O'Gorman P, McMillan DC, McArdle CS. Longitudinal study of weight, appetite, performance status, and inflammation in advanced gastrointestinal cancer. Nutr Cancer. 1999;35:127–9.
19. McMillan DC, Watson WS, O'Gorman P, Preston T, Scott HR, McArdle CS. Albumin concentrations are primarily determined by the body cell mass and the systemic inflammatory response in cancer patients with weight loss. Nutr Cancer. 2001;39:210–3.
20. O'Gorman P, McMillan DC, McArdle CS. Impact of weight loss, appetite, and the inflammatory response on quality of life in gastrointestinal cancer patients. Nutr Cancer. 1998;32:76–80.
21. Moyes LH, Leitch EF, McKee RF, Anderson JH, Horgan PG, McMillan DC. Preoperative systemic inflammation predicts postoperative infectious complications in patients undergoing curative resection for colorectal cancer. Br J Cancer. 2009;100:1236–9.
22. Huang TS, Hu FC, Fan CW, et al. A simple novel model to predict mortality, surgical site infection, and pneumonia in elderly patients undergoing operation. Dig Surg. 2010;27:224–31.

23. Miki C, Konishi N, Ojima E, Hatada T, Inoue Y, Kusunoki M. C-reactive protein as a prognostic variable that reflects uncontrolled up-regulation of the IL-1-IL-6 network system in colorectal carcinoma. Dig Dis Sci. 2004;49:970–6.
24. Ikeguchi M, Hatada T, Yamamoto M, Miyake T, Matsunaga T, Fukumoto Y, et al. Serum interleukin-6 and -10 levels in patients with gastric cancer. Gastric Cancer. 2009;12:95–100.
25. Chung YC, Chang YF. Serum interleukin-6 levels reflect the disease status of colorectal cancer. J Surg Oncol. 2003;83:222–6.
26. Gibbs J, Cull W, Henderson W, Daley J, Hur K, Khuri SF. Preoperative serum albumin level as a predictor of operative mortality and morbidity: results from the National VA Surgical Risk Study. Arch Surg. 1999;134:36–42.
27. Ryan AM, Hearty A, Prichard RS, Cunningham A, Rowley SP, Reynolds JV. Association of hypoalbuminemia on the first postoperative day and complications following esophagectomy. J Gastrointest Surg. 2007;11:1355–60.
28. Reynolds JV, Redmond HP, Ueno N, Steigman C, Ziegler MM, Daly JM, et al. Impairment of macrophage activation and granuloma formation by protein deprivation in mice. Cell Immunol. 1992;139:493–504.
29. Crumley AB, Stuart RC, McKernan M, McMillan DC. Is hypoalbuminemia an independent prognostic factor in patients with gastric cancer? World J Surg. 2010;34:2393–8.
30. Fearon KC, Falconer JS, Slater C, McMillan DC, Ross JA, Preston T. Albumin synthesis rates are not decreased in hypoalbuminemic cachectic cancer patients with an ongoing acute-phase protein response. Ann Surg. 1998;227:249–54.

Am J Transl Res 2014;6(3):179-187
www.ajtr.org /ISSN:1943-8141/AJTR1401006

Review Article

In vivo optical imaging of cancer metastasis using multiphoton microscopy: a short review

Koji Tanaka[1], Yuji Toiyama[1], Yoshinaga Okugawa[1], Masato Okigami[1], Yasuhiro Inoue[1], Keiichi Uchida[1], Toshimitsu Araki[1], Yasuhiko Mohri[1], Akira Mizoguchi[2], Masato Kusunoki[1]

Departments of [1]Gastrointestinal and Pediatric Surgery, [2]Neural Regeneration and Cell Communication, Mie University Graduate School of Medicine, 2-174 Edobashi, Tsu, Mie 514-8507, Japan

Received January 7, 2014; Accepted March 10, 2014; Epub May 15, 2014; Published May 30, 2014

Abstract: Intravital (in vivo) microscopy using fluorescently-tagged proteins is a valuable tool for imaging the expression of a specific protein, its subcellular location and the dynamics of specific cell populations in living animals. Recently, multiphoton microscopy including two-photon laser scanning microscopy (TPLSM) has been used in the field of tumor biology due to its ability to image target organs at higher magnification and at deeper depths from the tissue surface for longer time periods. We developed a method of *in vivo* real-time imaging for tumor metastasis using TPLSM with an organ stabilizing system, which allow us to observe not only a single tumor cell and its microenvironment for a long time, but also to observe the same organ of the same mouse at multiple time points in preclinical models. Here, we presented *in vivo* real-time images of 1) tumor cell arrest, 2) tumor cell-platelet interaction, 3) tumor cell-leukocyte interaction, and 4) metastatic colonization at the secondary organs as representative steps of metastatic process of experimental liver metastasis models using TPLSM.

Keywords: Cancer, metastasis, multiphoton microscopy

Introduction

Cancer is a major health problem worldwide. More than 90% of cancer patients will die from metastatic disease. Therefore, translational metastasis research should be prompted urgently [1]. The underlying mechanism of tumor metastasis has being investigated using molecular biology techniques intensively. Despite of accumulating evidence of molecular biological mechanisms underlying tumor metastasis, our comprehensive understanding is still unsatisfactory [2].

Metastatic process consists of a number of steps: the detachment of tumor cells from the primary tumor mass, intravasation into blood or lymphatic vessels, escape or avoidance from the host immune system, survival in the bloodstream, arrest at the secondary distant organs, extravasation of the arrested tumor cells through vessels, and successful colonization of tumor cells in the surrounding microenvironment different from the primary tumor [3]. The underlying mechanism of each step has been examined by *in vitro* and/or *in vivo* studies.

Imaging of living animals at microscopic resolution (intravital microscopy, IVM) represents a powerful tool for understanding the dynamics of metastatic process in the natural microenvironment [4, 5]. The development of suitable mouse models is also important for intravital imaging of metastatic process.

The dorsal skinfold window chamber model remains to be used widely for IVM of invasion, intravasation, metastasis process, and tumor angiogenesis of implantable tumor [6]. This model also makes it possible to take multiple imaging sessions over several days and months. Since then, mammary window chamber model for orthotopic breast tumor [7] and cranial window chamber model for brain tumor [8] have been also developed.

Intravital imaging of metastatic process using multiphoton microscopy

Multiphoton or two-photon laser scanning microscopy (TPLSM) utilizes two-photon excitation restricted to the focal plane by high-power, pulsed lasers. The longer-wavelengths as the

two-photon excitation source can penetrate deeper into tissues, up to 1000 μm [9]. The longer-(near-infrared) wavelengths can also reduce light scattering, resulting in an increased penetration depth. The two lower-energy excitation photons cause less photodamage, or phototoxicity (photobleaching). The absence of out-of-plane fluorescence can also contribute to the reduction of phototoxicity because of the two-photon excitation only at the focal plane [9]. TPLSM offers the above-mentioned numerous imaging benefits compared with single-photon confocal laser scanning microscopy (CLSM). Thus, TPLSM is thought to be an ideal tool for intravital imaging because of its ability to keep cell viability during imaging and to allow longer imaging time.

In vivo imaging of murine liver metastasis model using TPLSM

GFP-expressing mice

Enhanced green fluorescent protein (EGFP)-transgenic C57/BL6-Tg (CAG-EGFP) mice were purchased from Japan SLC Inc. (Sizuoka, Japan). GFP-expressing nude mice (C57BL/6-BALB/c-nu/nu-EGFP) were purchased from AntiCancer Japan (Osaka, Japan).

GFP mice (20-22 g) were bred, housed in groups of six mice per cage and fed with a pelleted basal diet (CE-7, CLEA Japan Inc., Tokyo, Japan). Mice had free access to drinking water. They were kept in the animal house facilities at Mie University School of Medicine under standard conditions of humidity (50 ± 10%), temperature (23 ± 2°C) and light (12/12 h light/dark cycle), according to the Institutional Animal Care Guidelines. The experimental protocols were reviewed and approved by the Animal Care and Use Committee at Mie University Graduate School of Medicine.

RFP-expressing cancer cell line

RFP expressing murine (SL4) and human (HT-29) cancer cell lines were purchased from AntiCancer Japan (Osaka, Japan).

The inoculation of RFP-SL4 cells in GFP mice was used as a syngeneic tumor model. By contrast, the inoculation of RFP-HT29 cells in GFP nude mice was used as a xenogeneic tumor model.

Cancer cells were grown in monolayer cultures in RPMI 1640 (Sigma-Aldrich, Inc., St. Louis, MO. USA) supplemented with fetal bovine serum (FBS, 10% (v/v), GIBCO BRL, Tokyo, Japan), glutamine (2 mM), penicillin (100000 units/liter), streptomycin (100 mg/liter), and gentamycin (40 mg/liter) at 37°C in a 5% CO_2 environment. For routine passage, cultures were spilt 1:10 when they reached 90% confluence, generally every 3 days. Cells at the fifth to ninth passage were used for liver metastasis experiments, which were performed with exponential growing cells.

Murine liver metastasis model

RFP-expressing cancer cells were inoculated into the spleens of GFP mice, as a colorectal liver metastatic xenograft model [10]. RFP-HT29 or RFP-SL4 cancer cells at the fifth to ninth passage were harvested with trypsin/EDTA, and washed in serum-containing RPMI 1640 medium to inactivate any remaining trypsin. The cells were centrifuged and resuspended in phosphate-buffered saline (PBS). Finally, the cells were adjusted to 2×10^7 cells/mL for single cell suspensions.

GFP mice were anaesthetized using an anaesthetic mask with 4 L/min of isofluorane (4%; Forane, Abbott, Japan). Anaesthetic maintenance was achieved using 1.5-2% isoflurane and 4 L/min of O_2. Under direct vision, 2×10^6 cells were injected into the spleen using a 30-gauge needle through a small incision in the left lateral abdomen of anesthetized GFP mice.

Liver stabilization for *in vivo* imaging using TPLSM

Previously we have reported a method of *in vivo* real-time imaging for various murine models using TPLSM with an organ stabilizing system, which allows high magnification (×600 or higher) and high resolution (at the cellular or subcellular level) images in living animals [11-17].

Figure 1A shows an overview of liver stabilization for in vivo imaging using TPLSM. The upper midline laparotomy was made (< 15 mm) in the anaesthetized mice. The left lateral lobe of the liver was identified and exteriorized through the laparotomy (**Figure 1B**). The liver lobe was then put onto a solder lug terminal with an instant adhesive agent (KO-10-p20, DAISO, Japan)

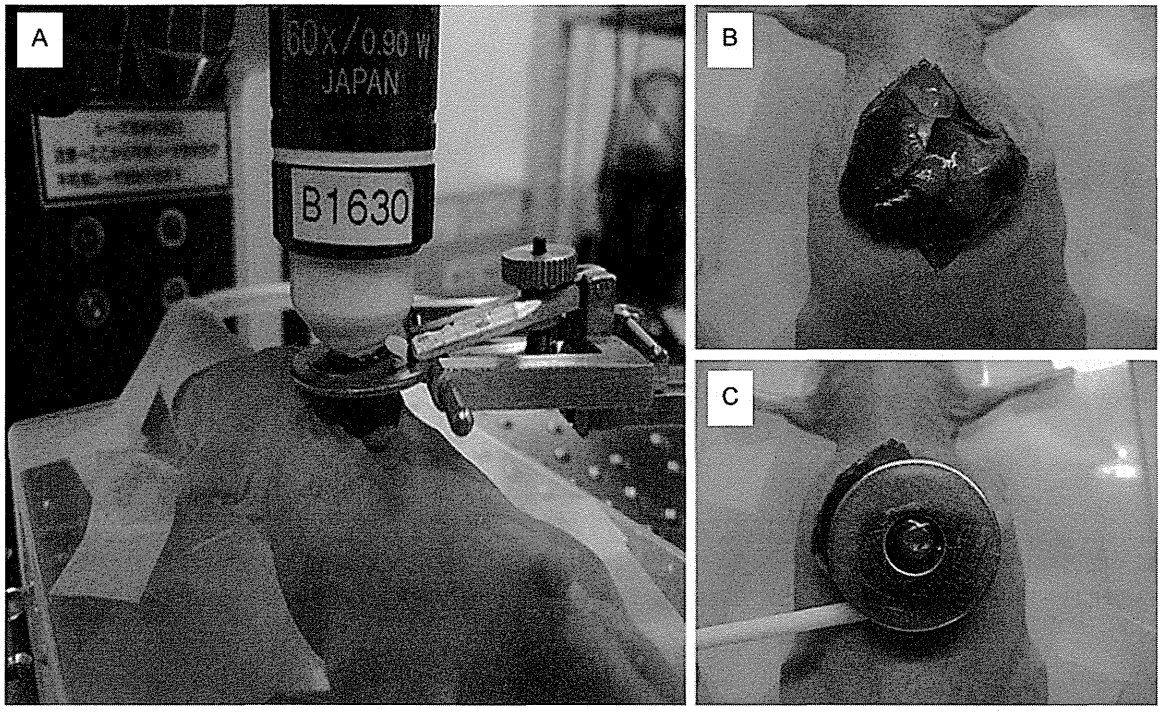

Figure 1. Overview of liver stabilization for *in vivo* imaging using TPLSM: A. Overview of liver stabilization using organ stabilizing system; B. Exteriorization of liver lobes; C. Liver stabilization using a solder lug terminal.

(**Figure 1C**). This organ stabilizer minimized the microvibration of the observed area caused by physiological heart beat and respiratory movements. After the application of PBS to the observed area, a thin cover glass was placed on the liver surface. After intravital TPLSM, a solder lug terminal was removed from the liver lobe using a release agent (KO-10-p8, DAISO, Japan). The liver surface were extensively washed by PBS to remove the residual release agent and blood coagulation mass. A sodium hyaluronate and carboxymethylcellulose membrane (Seprafilm Adhesion Barrier, Genzyme Corporation, Cambridge, MA) was placed between the liver and the abdominal wall to prevent postoperative dense adhesion. Body temperature was kept at 37°C throughout the experiments using a heating pad. Normal saline (200 μL) were administered intraperitoneally at 1-2 hour intervals for hydration during anesthesia.

TPLSM setup

The detailed procedures for TPLSM setup were described as previously [14]. In brief, experiments were performed using an upright microscope (BX61WI; Olympus, Tokyo, Japan) and a FV1000-2P laser-scanning microscope system (FLUOVIEW FV1000MPE, Olympus, Tokyo, Japan). The use of special stage risers enabled the unit to have an exceptionally wide working distance. This permitted the stereotactically immobilized, anesthetized mouse to be placed on the microscope stage. The microscope was fitted with several lenses with high numeric apertures to provide the long working distances required for *in vivo* work, and with water-immersion optics. The excitation source in TPLSM mode was Mai Tai Ti: sapphire lasers (Spectra Physics, Mountain View, CA), tuned and mode-locked at 910 nm. The Mai Tai produces light pulses of about 100 fs width (repetition rate 80 MHz). Laser light reached the sample through the microscope objectives, connected to an upright microscope (BX61WI; Olympus, Tokyo, Japan). A mean laser power at the sample was between 10 and 40 mW, depending on the depth of imaging. Microscope objective lens were 4×UPlanSApo (numerical aperture of 0.16), 10×UPlanSApo (numerical aperture of 0.4), and 60×LUMPlanFI/IR (water dipping, numerical aperture of 0.9, working distance 2 mm), respectively. Data were analyzed using a FV10-ASW (Olympus, Tokyo, Japan). TPLSM images were acquired with 512×512 pixels

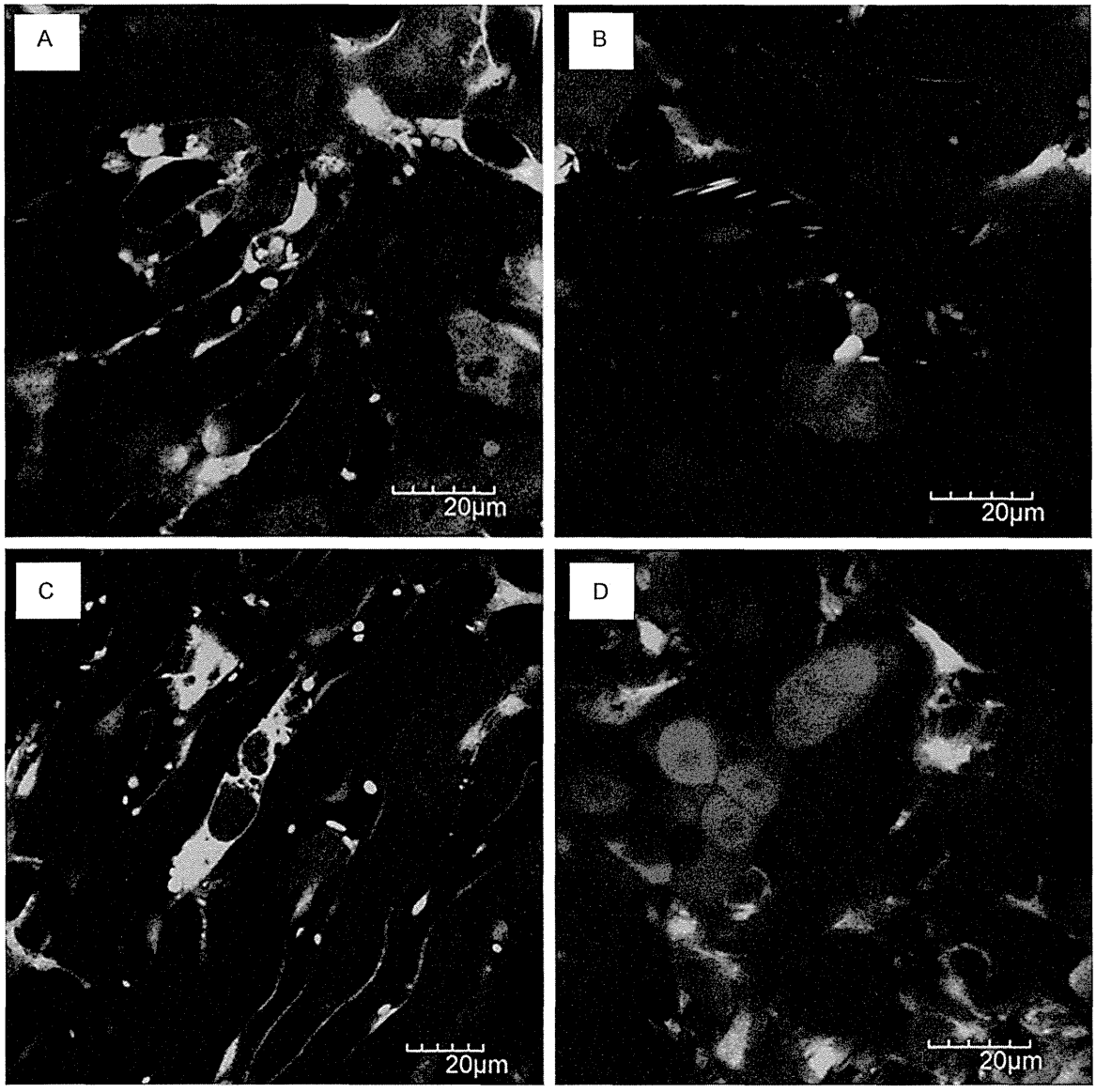

Figure 2. Visualization of liver metastatic process in xenogenic model: A. Tumor cell-platelet interaction; B. Tumor cell-leukocyte interaction; C. Platelets aggregation to the tumor cell; D. Liver metastatic colonization.

spatial resolution, from 210 μm field of view dimension, using a pixel dwelling time 4 μs. Two-photon fluorescence signals were collected by an internal detector (non-descanned detection method) at an excitation wavelength, to enable the simultaneous acquisition of EGFP signal and RFP (DsRed2) signal. Color-coded green and red images were imaged at the same time, and subsequently merged to produce single images.

Imaging methods

The surface of the liver was screened at lower magnifications by setting out the X/Y plane and adjusting the Z axis manually to detect the optimal observation area containing RFP-expressing cancer cells (at least five areas). Subsequently, each area of interest was scanned at a higher magnification (water-immersion objective 60× with or without 2× zoom) by manually setting the X/Y plane and adjusting the Z axis either automatically or manually. The scanning areas were 200×200 μm (600×) or 100×100 μm (600× with 2× zoom) respectively. The imaging depth was determined arbitrarily. The laser power was adjusted according to the imaging depth. When imaging at larger depths, we increase the laser power level (up to near 100%) manually using laser power level

controller. To image the optimal simultaneous imaging of EGFP and RFP (DsRed2), detection sensitivity (brightness by HV) was adjusted manually for EGFP (450-500) or RFP (550-600), respectively.

Visualization of liver metastatic process in xenogenic model (HT29)

Injection in the spleen or portal vein mimics hematogenous spread of tumor cells into the liver, which has been used by many researchers to create liver metastases. Tumor cells which were injected into the spleen circulated in the bloodstream (portal route), and then get stuck (or arrested) in the hepatic sinusoids. We can observe metastatic processes such as the tumor cell arrest, tumor endothelial interaction, tumor cell extravasation into the liver parenchyma, and the metastatic colonization in the liver using a liver metastasis model by intrasplenic injection of tumor cells.

Tumor cell arrest

In our study, red-colored cancer cells were visualized in the green-colored liver structures of GFP mice at the single cell level (at a magnification of over 600×). Cancer cells were arrested in hepatic sinusoids 2 hours after injection. Circulating or rolling cancer cells in hepatic vessels were never observed during the 1 hour observation time. However, cancer cells appeared to gather into the central zone of hepatic lobes. It still remains unclear whether tumor cell arrest might be caused by molecular adhesion between cancer cells and hepatic endothelial cells or size-dependent occlusion.

Tumor cell-platelet interaction

Figure 2A shows a tumor cell-platelet interaction within hepatic sinusoids. In GFP mice, red blood cells were not visualized [18]. Therefore, leukocytes were recognized as larger blood cells, and platelets were recognized as smaller ones within blood vessels. Within hepatic sinusoids, we observed that leukocytes including Kupffer cells were rolling or flowing *in vivo* real-time.

The fact that platelets are essential for hematogenous tumor metastasis has been demonstrated more than 4 decades ago and has been proven in a lot of experiments [19-21]. The interaction of tumor cells with platelets within the bloodstream occurs from the moment of tumor cell entry into the bloodstream (intravasation) to the moment that tumor cells leave from blood vessels (extravasation). Tumor cell induced platelet aggregation (TCIPA) is the phenomenon of which tumor cells can aggregate platelets. The advantageous role of TCIPA for tumor metastasis is thought to be the prolongation of tumor cell survival in the bloodstream and the protection of tumor cell by surrounding platelets from host immune system.

We observed in vivo real-time that platelets adhered to the intrasinusoidal (intravascular) tumor cells under normal blood flow, indicating a tumor cell-platelet interaction. **Figure 2C** also showed that platelets aggregated to the intrasinusoidal tumor cells like a protective coat. We think that it is thought to be a intravital imaging of TCIPA at high magnification and high resolution.

Tumor cell-leukocyte interaction

Figure 2B shows a tumor cell-leukocyte interaction. The increase in neutrophil counts or neutrophil-to-lymphocyte ratios has demonstrated to be predictive value of poor prognosis or distant metastasis in several human malignancies [22, 23]. The presence of circulating tumor cells (CTC) has been shown to be a surrogate biomarker of hematogenous metastases [24, 25]. There is increasing evidence of CTC-neutrophil interaction in vitro. The role of neutrophils in CTC recruitment to the metastatic organs has been also reported [26, 27]. The interaction between tumor cells and neutrophils is thought to play an important role in tumor metastatic cascade.

We observed that leukocytes adhered to tumor cells within hepatic sinusoids *in vivo* real-time. We previously reported an intravital imaging of a leukocyte with ameboid morphology capturing a cancer cell [14]. The leukocyte with reticular protrusions is thought to phagocytose cancer cells in hepatic sinusoids. It remains unknown whether the interaction between neutrophils and intravascular tumor cells may be related to promote metastatic colonization by enhancing tumor cell extravasation following tumor cell-endothelial interaction or to suppress tumor metastasis by phagocytosing CTCs.

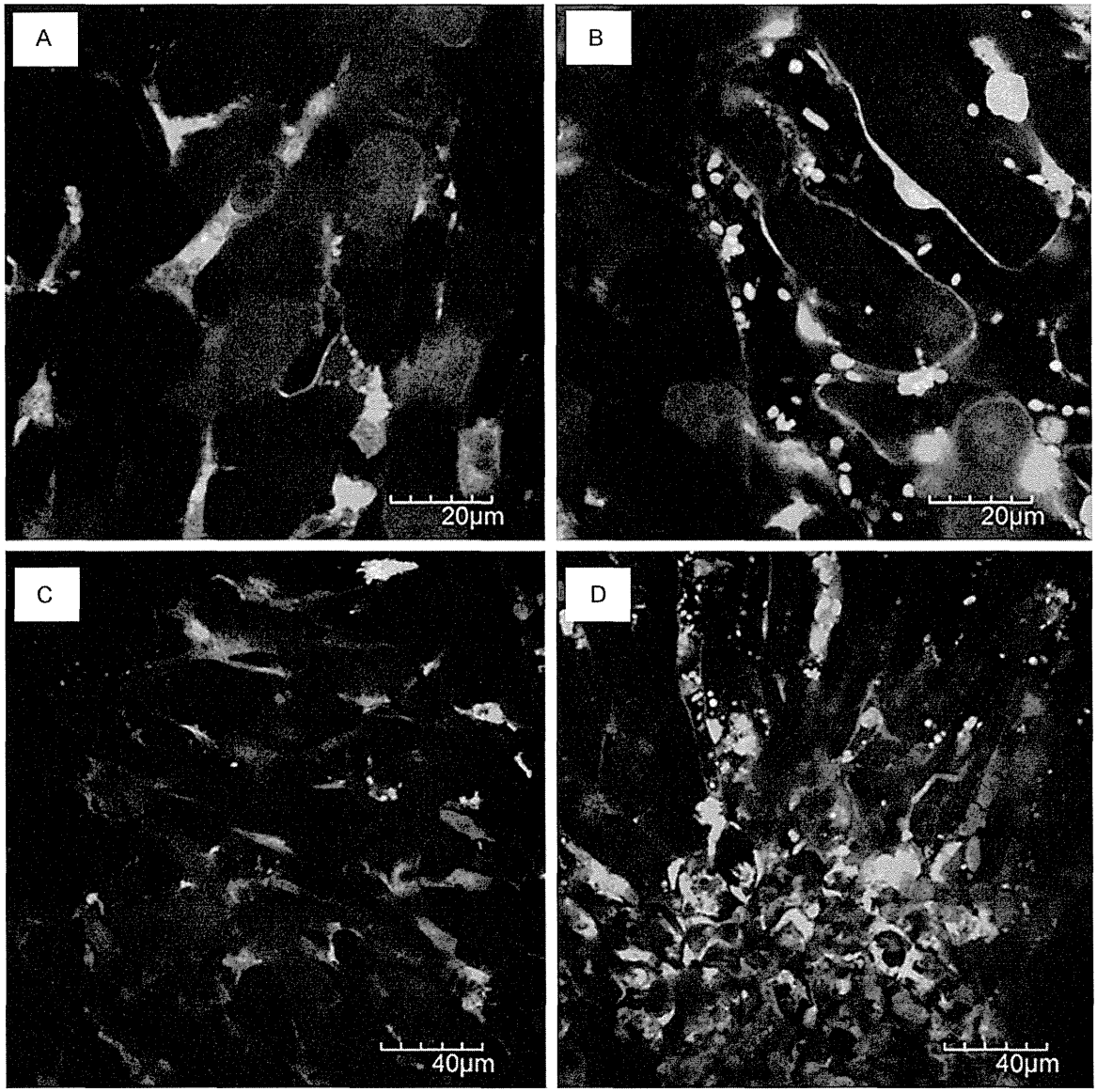

Figure 3. Visualization of liver metastatic process in syngeneic model: A. Tumor cell arrest; B. Tumor cell extravasation; C. Liver metastatic colonization showing diffuse growth pattern; D. Liver metastatic colonization with extensive stromal reaction.

Metastatic colonization at the secondary organs

It has been the challenge for long time to image *in vivo* real-time the development of micrometastases at the secondary distant organs such as liver, lung, and brain using TPLSM because of motion artifact due to cardiac and respiratory movement.

We developed a method of *in vivo* real-time TPLSM imaging for experimental metastasis models using an organ stabilizing system, which allows to observe several steps of metastatic cascade at high magnification (×600 or higher) and high resolution (at the cellular or subcellular level) in living animals [14-17].

We also developed a method of time-series (at multiple time points) intravital TPLSM imaging in the same mice over the long experimental periods by the prevention of abdominal adhesions using a sodium hyaluronate and carboxymethylcellulose membrane (Seprafilm Adhesion Barrier, Genzyme Corporation, Cambridge, MA). Time-series intravital TPLSM imaging allow to

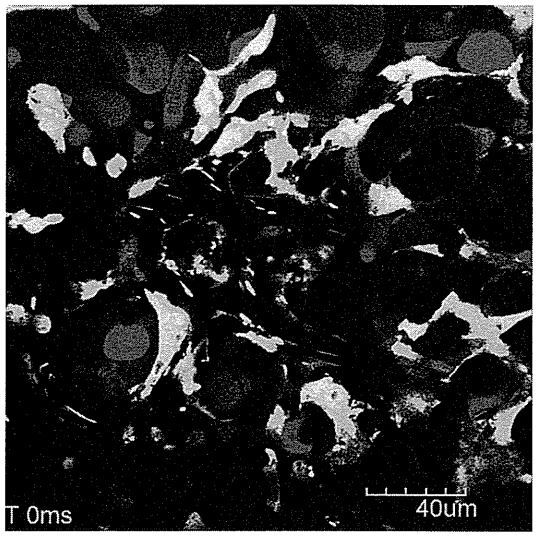

Figure 4. Tumor vessels of liver metastatic xenografts. Supplementary movie shows a time lapse imaging of a blood flow in the tumor vessels of liver metastatic xenografts.

image liver metastatic xenografts of the same mice until the formation of non-dissecting adhesions between the liver and the abdominal wall. We can take time-series images of liver metastatic xenografts in the same mice up to three time points.

Figure 2D shows a metastatic colonization of RFP-HT29 cells in the liver 2 month after the injection of tumor cells directly into the spleen. Liver metastases of RFP-HT29 showed multiple metastatic nodules macroscopically. Each metastatic nodule showed multiple micrometastatic clusters consisting of several tumor cells microscopically.

We couldn't observe the metastasis formation process continuously from a single tumor cell to micrometastatic colonization at the secondary organ because it is impossible to continue intravital TPLSM over 24 hours due to surgical stress by liver exteriorization. Therefore, it remains to be determined whether a single tumor cell retains as dormant state for long time or tumor cells directly proliferate within hepatic sinusoids (intravascular proliferation) or they proliferate in the liver parenchyma after the extravasation through hepatic endothelial cells [28].

Visualization of liver metastatic process in syngeneic model (SL4)

Tumor transplantation models of metastasis require the inoculation of human (xenograft/xenogenic) or mouse (allograft/syngeneic) cells/tissue into murine hosts. Experimental metastasis models by either xenogenic or syngenic tumor involve the injection of tumor cells directly into the vascular system, which skip the formation of a primary tumor (orthotopically or ectopically) and the invasion into the local environment. Because murine tumor cells are inoculated into the immunocompetent hosts with the same species and genetic background, syngeneic tumor models provide a valuable preclinical tool of intact tumor-host interaction by intact immune systems in the metastatic cascade.

Similar to xenogenic tumor metastasis model using RFP-HT29, tumor cell arrest (**Figure 3A**), tumor cell-platelet interaction, tumor cell-leukocyte interaction, and metastatic colonization at the secondary organs (**Figure 3C, 3D**) were observed *in vivo* real-time in syngeneic tumor metastasis model using RFP-SL4.

The space between hepatic endothelial cells and hepatocytes is named as the space of Disse (or perisinusoidal space). Spindle-shaped RFP-SL4 cells were localized in this space (**Figure 3B**). As shown in **Figure 3A**, RFP-SL4 cells are round-shaped just after intrasplenic injection. Thus, spindle-shaped RFP-SL4 cells were thought to be extravasated from hepatic sinusoids to the space of Disse 24 hours after injection.

However, we couldn't observe *in vivo* real-time the process of change in tumor cell morphology from a round-shape into a spindle-shape and the moment of intravascular tumor cells extravasate into liver parenchyma via vascular endothelium.

Figure 2D shows a metastatic colonization of RFP-HT29 cells in the liver 2 month after the injection of tumor cells directly into the spleen. Liver metastases of RFP-SL4 showed diffusely infiltrative growth macroscopically 14 days after the injection of tumor cells directly into the spleen. Microscopically, RFP-SL4 cells proliferated diffusely with extensive stromal reaction (**Figure 3C, 3D**).

Direct visualization of metastatic process at the secondary organs by TPLSM

Intravital TPLSM imaging using an organ stabilizing system can allow us to visualize each step

of metastatic cascade at high magnification and high resolution in living animals [14-17].

Time-series intravital TPLSM imaging can also allow us to visualize the same organ of the same animal at multiple time points (up to three times) during the long experimental periods. Therefore, we can directly visualize metastatic process at the secondary organs at high magnification and high resolution at least three times.

We presented *in vivo* real-time images of 1) tumor cell arrest, 2) tumor cell-platelet interaction, 3) tumor cell-leukocyte interaction, and 4) metastatic colonization at the secondary organs as representative steps of metastatic process of experimental liver metastasis models.

The spatiotemporal interactions between tumor cells and host cells during metastatic process can be visualized by using time-lapse and z-stacks imaging [14, 17]. **Figure 4** (supplementary movie 1) shows a blood flow in the tumor vessels of liver metastatic xenografts. As previously reported [15, 16], the interaction between intravascular tumor cells and endothelial cells or blood cells except for erythrocytes can be also observed. Platelet aggregation in tumor vessels and the adhesion of platelet aggregation to tumor endothelial cells were observed as the intravascular abnormalities within liver metastatic xenografts.

Although direct visualization of metastatic process at the secondary organs in vivo real-time might be valuable, there are still several issues which should be overcome. We must try to visualize the moment of each step of metastatic cascade at high magnification and high resolution in living animals. In our procedure, we couldn't observe the metastasis formation process continuously from a single tumor cell to micrometastatic colonization. We couldn't also observe the moment of change in tumor cell morphology or the moment of metastatic colonization by tumor cell division.

Direct visualization of metastatic process by real-time imaging for extended periods (over 24 hours per session) will help us to understand the spatiotemporal tumor-host interaction on tumor metastasis at the cellular and subcellular levels.

Disclosure of conflict of interest

None.

Address correspondence to: Koji Tanaka, Department of Gastrointestinal and Pediatric Surgery, Mie University Graduate School of Medicine, 2-174 Edobashi, Tsu, Mie 514-8507, Japan. Tel: 81-59-231-5294; Fax: 81-59-232-6968; E-mail: qouji@clin.medic.mie-u.ac.jp

References

[1] Sleeman J, Steeg PS. Cancer metastasis as a therapeutic target. Eur J Cancer 2010; 46: 1177-80.

[2] Valastyan S, Weinberg RA. Tumor metastasis: molecular insights and evolving paradigms. Cell 2011; 147: 275-92.

[3] Mathot L, Stenninger J. Behavior of seeds and soil in the mechanism of metastasis: a deeper understanding. Cancer Sci 2012; 103: 626-31.

[4] Pittet MJ, Weissleder R. Intravital imaging. Cell 2011; 147: 983-91.

[5] Beerling E, Ritsma L, Vrisekoop N, Derksen PW, van Rheenen J. Intravital microscopy: new insights into metastasis of tumors. J Cell Sci 2011; 124: 299-310.

[6] Hak S, Reitan NK, Haraldseth O, de Lange Davies C. Intravital microscopy in window chambers: a unique tool to study tumor angiogenesis and delivery of nanoparticles. Angiogenesis 2010; 13: 113-30.

[7] Kedrin D, Gligorijevic B, Wyckoff J, Verkhusha VV, Condeelis J, Segall JE, van Rheenen J. Intravital imaging of metastatic behavior through a mammary imaging window. Nat Methods 2008; 5: 1019-21.

[8] Kienast Y, von Baumgarten L, Fuhrmann M, Klinkert WE, Goldbrunner R, Herms J, Winkler F. Real-time imaging reveals the single steps of brain metastasis formation. Nat Med 2010; 16: 116-22.

[9] Ustione A, Piston DW. A simple introduction to multiphoton microscopy. J Microsc 2011; 243: 221-6.

[10] de Jong GM, Aarts F, Hendriks T, Boerman OC, Bleichrodt RP. Animal models for liver metastases of colorectal cancer: research review of preclinical studies in rodents. J Surg Res 2009; 154: 167-76.

[11] Toiyama Y, Mizoguchi A, Okugawa Y, Koike Y, Morimoto Y, Araki T, Uchida K, Tanaka K, Nakashima H, Hibi M, Kimura K, Inoue Y, Miki C, Kusunoki M. Intravital imaging of DSS-induced cecal mucosal damage in GFP-transgenic mice using two-photon microscopy. J Gastroenterol 2010; 45: 544-53.

[12] Koike Y, Tanaka K, Okugawa Y, Morimoto Y, Toiyama Y, Uchida K, Miki C, Mizoguchi A, Kusunoki M. In vivo real-time two-photon microscopic imaging of platelet aggregation induced by selective laser irradiation to the endothelium created in the beta-actin-green fluorescent protein transgenic mice. J Thromb Thrombolysis 2011; 32: 138-45.
[13] Morimoto Y, Tanaka K, Toiyama Y, Inoue Y, Araki T, Uchida K, Kimura K, Mizoguchi A, Kusunoki M. Intravital three-dimensional dynamic pathology of experimental colitis in living mice using two-photon laser scanning microscopy. J Gastrointest Surg 2011; 15: 1842-50.
[14] Tanaka K, Morimoto Y, Toiyama Y, Okugawa Y, Inoue Y, Uchida K, Kimura K, Mizoguchi A, Kusunoki M. Intravital dual-colored visualization of colorectal liver metastasis in living mice using two photon laser scanning microscopy. Microsc Res Tech 2012; 75: 307-15.
[15] Tanaka K, Morimoto Y, Toiyama Y, Matsushita K, Kawamura M, Koike Y, Okugawa Y, Inoue Y, Uchida K, Araki T, Mizoguchi A, Kusunoki M. In vivo time-course imaging of tumor angiogenesis in colorectal liver metastases in the same living mice using two-photon laser scanning microscopy. J Oncol 2012; 2012: 265487.
[16] Tanaka K, Okigami M, Toiyama Y, Morimoto Y, Matsushita K, Kawamura M, Hashimoto K, Saigusa S, Okugawa Y, Inoue Y, Uchida K, Araki T, Mohri Y, Mizoguchi A, Kusunoki M. In vivo real-time imaging of chemotherapy response on the liver metastatic tumor microenvironment using multiphoton microscopy. Oncol Rep 2012; 28: 1822-30.
[17] Tanaka K, Toiyama Y, Inoue Y, Uchida K, Araki T, Mohri Y, Mizoguchi A, Kusunoki M. Intravital imaging of gastrointestinal diseases in preclinical models using two-photon laser scanning microscopy. Surg Today 2013; 43: 123-9.
[18] Okabe M, Ikawa M, Kominami K, Nakanishi T, Nishimune Y. 'Green mice' as a source of ubiquitous green cells. FEBS Lett 1997; 407: 313-9
[19] Erpenbeck L, Schön MP. Deadly allies: the fatal interplay between platelets and metastasizing cancer cells. Blood 2010; 115: 3427-36.
[20] Gay LJ, Felding-Habermann B. Contribution of platelets to tumour metastasis. Nat Rev Cancer 2011; 11: 123-34.
[21] Buergy D, Wenz F, Groden C, Brockmann MA. Tumor-platelet interaction in solid tumors. Int J Cancer 2012; 130: 2747-60.
[22] Ubukata H, Motohashi G, Tabuchi T, Nagata H, Konishi S, Tabuchi T. Evaluations of interferon-γ/interleukin-4 ratio and neutrophil/lymphocyte ratio as prognostic indicators in gastric cancer patients. J Surg Oncol 2010; 102: 742-7.
[23] Liu H, Liu G, Bao Q, Sun W, Bao H, Bi L, Wen W, Liu Y, Wang Z, Yin X, Bai Y, Hu X. The baseline ratio of neutrophils to lymphocytes is associated with patient prognosis in rectal carcinoma. J Gastrointest Cancer 2010; 41: 116-20.
[24] Yu M, Stott S, Toner M, Maheswaran S, Haber DA. Circulating tumor cells: approaches to isolation and characterization. J Cell Biol 2011; 192: 373-82.
[25] Ghadially R. The role of stem and circulating cells in cancer metastasis. J Surg Oncol 2011; 103: 555-7.
[26] Huh SJ, Liang S, Sharma A, Dong C, Robertson GP. Transiently entrapped circulating tumor cells interact with neutrophils to facilitate lung metastasis development. Cancer Res 2010; 70: 6071-82.
[27] Spicer JD, McDonald B, Cools-Lartigue JJ, Chow SC, Giannias B, Kubes P, Ferri LE. Neutrophils promote liver metastasis via Mac-1-mediated interactions with circulating tumor cells. Cancer Res 2012; 72: 3919-27.
[28] Robertson JH, Sarkar S, Yang SY, Seifalian AM, Winslet MC. In vivo models for early development of colorectal liver metastasis. Int J Exp Pathol 2008; 89: 1-12.

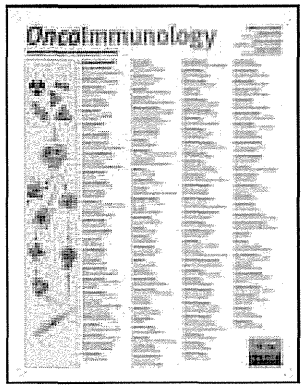

OncoImmunology
Publication details, including instructions for authors and subscription information:
http://www.tandfonline.com/loi/koni20

Antibody response to cancer/testis (CT) antigens: A prognostic marker in cancer patients

Yoshihiro Ohue[a], Hisashi Wada[b], Mikio Oka[a] & Eiichi Nakayama[c]

[a] Department of Respiratory Medicine; Kawasaki Medical School; Kurashiki, Japan

[b] Department of Clinical Research in Tumor Immunology; Graduate School of Medicine; Osaka University; Suita, Japan

[c] Faculty of Health and Welfare; Kawasaki University of Medical Welfare; Kurashiki, Japan

Accepted author version posted online: 10 Dec 2014.Published online: 21 Dec 2014.

To cite this article: Yoshihiro Ohue, Hisashi Wada, Mikio Oka & Eiichi Nakayama (2014) Antibody response to cancer/testis (CT) antigens: A prognostic marker in cancer patients, OncoImmunology, 3:11, e970032, DOI: 10.4161/21624011.2014.970032

To link to this article: http://dx.doi.org/10.4161/21624011.2014.970032